
DELIVERABLE

D.4.3

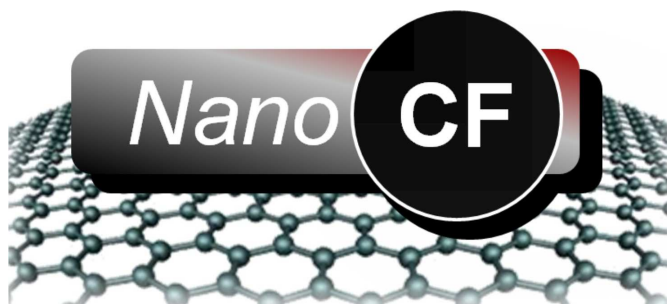
Interpretation of resonance Raman spectra of fluorinated carbon nanomaterials

Grant Agreement number: 612577

Project acronym: NanoCF

Project title: Tuning the properties of NanoCarbon with Fluorination

Funding Scheme: FP7-MC-IRSES



Project coordinator name: Dr. Ulrich Scheler

Tel: +49 351 4658 275

Fax: +49 351 4658 231

E-mail: scheler@ipfdd.de

Project coordinator organization name: Leibniz-Institut für Polymerforschung Dresden e.V.

Project website address: www.nanocf.eu

Work Package nr. from Annex I: 4

Deliverable nr. from Annex I: 4.3

Title: Interpretation of resonance Raman spectra of fluorinated carbon nanomaterials

Related to a reporting period: 2

Reporting Period: 1.10.2015-30.09.2017

Lead beneficiary: CNRS

Nature: Report

Dissemination Level: UE level

Delivery date from Annex I: month 36

Deliverable Document Type: report

The reported work was done in the framework of Task 4.3 Interpretation of resonance Raman spectra of fluorinated carbon nanomaterials (IBCH SB RAS, key person: Ekaterina Obraztsova).

Raman spectra of graphite and fluorinated graphite flakes are presented in Figure 1. As reported in literature fluorographene shows good chemical and thermal stability as a result of strong C-F bonding energy [Feng, *Advanced Science*, 3, 2016]. We could thus utilize Raman spectroscopy to study fluorinated graphene because it can provide a wealth of information about the structures of graphene-based materials. We have found that high intensities of excitation laser illumination can lead to sufficient for defluorination heating. Typical spectrum of fluorinated graphite consists of standard G, D and 2D peaks. However, the increased intensity of disorder induced D line and the lines width indicate that a high degree of structural disorder was introduced during the fluorination.

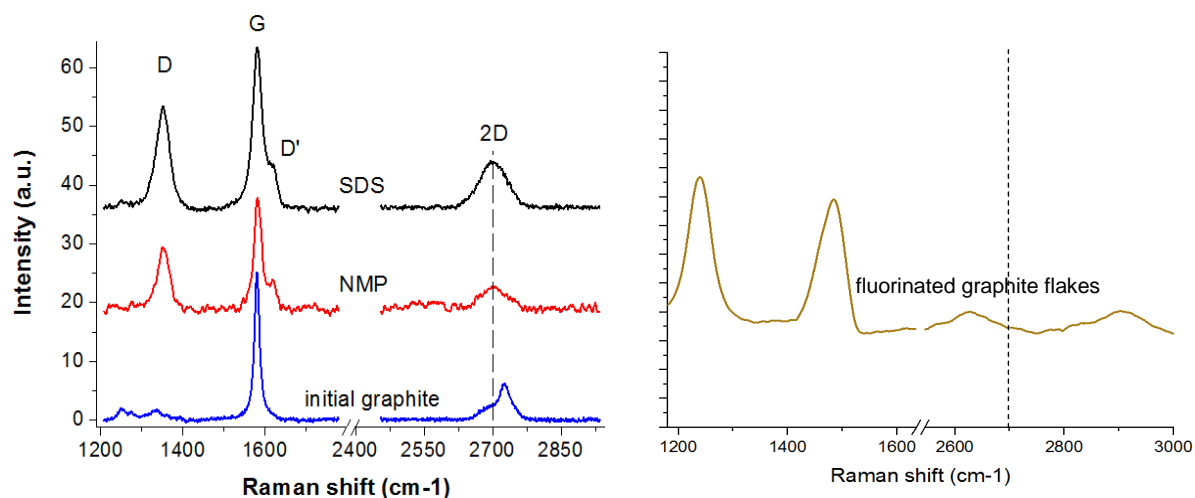


Figure 1. Raman spectra of graphite and graphene flakes in comparison with fluorinated graphite.

Bromination of fluorinated carbon nanotubes

Drawing on our understanding of fluorinated carbon nanotubes, we extended this work to use fluorination as a probe to investigate the behaviour of further halogen treatments on carbon nanomaterials. In particular, bromine treatment of carbon nanotubes has been proposed as a different way to induce non-destructive doping of the nanotube network. In addition it is an approach we use for separating graphene from graphite samples, via bromine intercalation. A detailed understanding of the bromination process is therefore essential, and it is difficult to evaluate from purely Raman spectroscopy studies of brominated pristine nanocarbon samples.

For this reason bromination of DWCNT samples was carried out with gaseous mixture of BrF_3 and Br_2 at room temperature, by our Siberian partner in Novosibirsk, using double walled carbon nanotubes produced by Partner CNRS in Toulouse. The resultant data was then taken to Partner CNRS in Nantes during a recent exchange, where a further sequence of theoretical modelling was used to successfully interpret the bromine signals as follows.

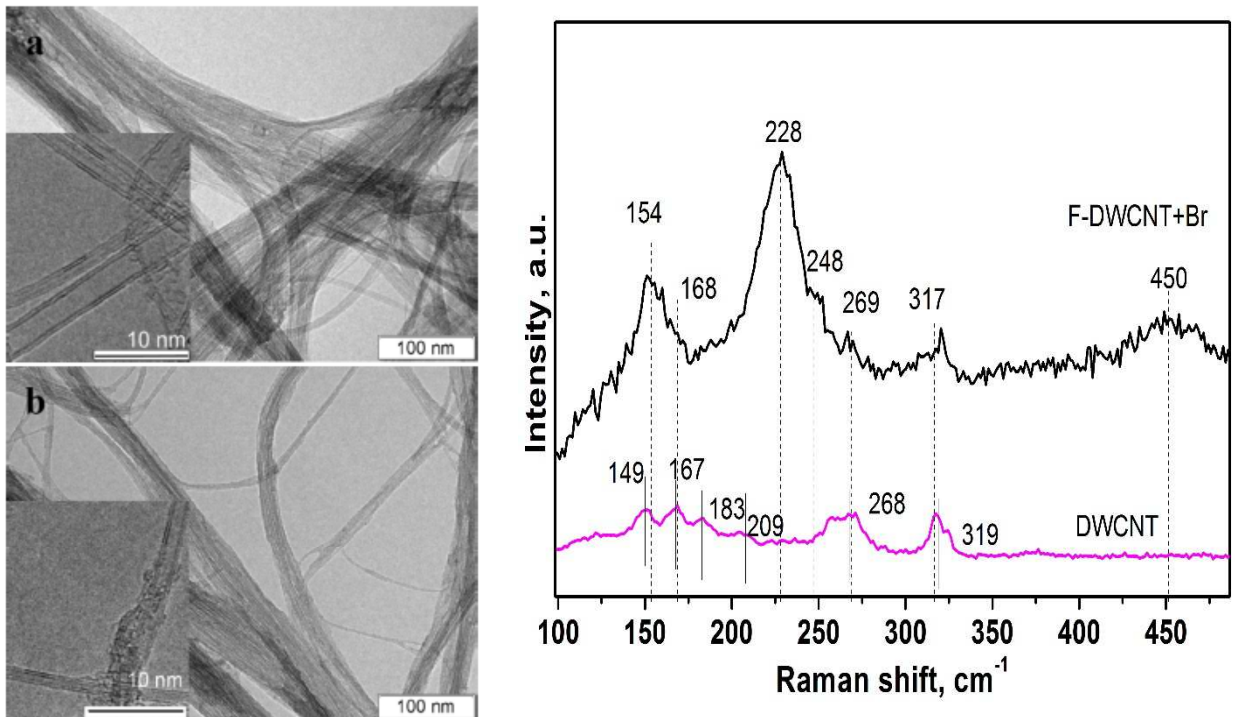


Figure 2. (left) TEM images of pristine DWCNTs (a) and brominated DWCNTs (b). The inset shows the individual DWCNTs that occur in the sample. (right) Raman spectra taken with 514 nm laser excitation energy for pristine DWCNTs and brominated DWCNTs (c).

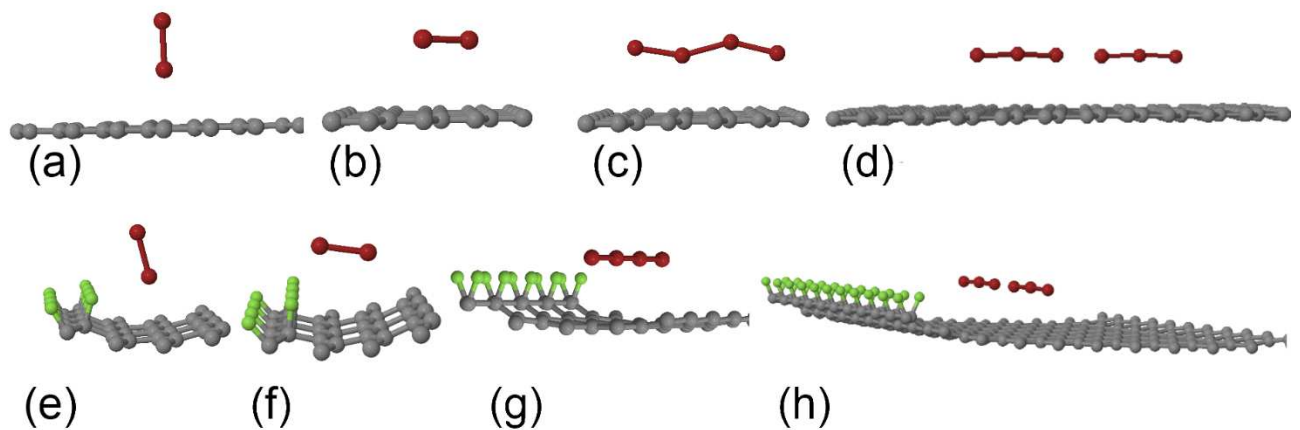


Figure 3. Optimized geometries of Br₂ oriented perpendicular (a, e) and parallel (b, f) to a graphene and fluorinated graphene sheets. Optimized geometries of Br₄ (c, g) and Br₆ (d, h) molecules oriented parallel to a graphene and fluorinated graphene sheets.

Figure 2 shows TEM imagery of the nanotube samples before and after bromination treatment. XPS data shows that the fluorination process leads to partial banded coverage of the nanotube surface. The Raman signal pre-bromination in the 100-450cm⁻¹ range shows a range of bands due to the radial breathing motion in the carbon nanotubes.

However after fluorination and bromination these bands are no longer present and instead the spectrum is dominated by a sequence of bands, primarily at 154cm^{-1} and 228cm^{-1} (bands at 317 and 450cm^{-1} are overtone bands). Through a sequence of DFT atomistic models we have been able to show (Figure 3) that while Bromine molecules (Br_2) sit preferentially orthogonal to the carbon surface (e.g. graphene or nanotube surface), once multiple bromine molecules are present, they spontaneously (with no energetic barrier) combine. A combination to Br_4 requires a small barrier and is weakly energetically favoured, however three Br_2 molecules combine to give two coupled Br_3 molecules with no barrier and large release in energy. These Bromine chains appear exceptionally stable and give rise to the Raman vibrational modes seen in experiment (see Table 1). This represents a successful interpretation of the experimental data and is the first time that such bromine chains have been unambiguously proposed and identified in the literature. They are important since Br_3 results in much stronger charge transfer and doping effects than Br_2 molecules, and hence this suggests that Bromine addition may be an exceptionally efficient route to electronic doping of carbon nanomaterials, and successful doping of this nature can be identified by the presence notably of Raman peaks at 154 and 228cm^{-1} . These results are quite new and we are now in the process of preparing a paper on this finding.

Table 1. Calculated properties of graphene and fluorinated graphene interacting with different bromine species

| | Graphene | | | | Fluorinated Graphene | | | |
|--|-----------------|------------|---|---|----------------------|------------|---|---|
| | Br ₂ | | Br ₄ | Br ₆ | Br ₂ | | Br ₄ | Br ₆ |
| | ⊥ | ∥ | | | ⊥ | ∥ | | |
| Binding energy / Br _n (eV) | -0.20 | -0.12 | -0.27 | -0.65 | -0.17 | -0.24 | -0.34 | -0.55 |
| Total charge transfer / Br _n (e) | -0.13 | -0.12 | -0.21 | -1.28 | -0.08 | -0.20 | -0.21 | 1.25 |
| Br-Br stretching Frequency (cm ⁻¹) | 281.8 (ss) | 265.9 (ss) | 199.2 (ss); 149.9 (bv); 80.2 (l); 41.3 | 223.1 (ss); 158.7 (ss); 82 (bv); 73.2 (bv); 69.9 (bv); 59.5 (eV) | 300.7 (ss) | 322.0 (ss) | 236.5 (st), 142.1 (bv); 88.9 (bv); 62.7 (bv) | 224.5 (ss); 159.4 (ss); 85.7 (bv); 72.1 (bv); 71.8 (bv); 59.1 (bv) |

Fluorinated DWCNTs have been synthesized in the framework of Task 2.3 Room- and high-temperature fluorination (NIIC SB RAS, key person: Lyuba Bulusheva) and Task 2.4 Plasma fluorination (UMONS, key person: Carla Bittencourt). Raman spectra of the samples were measured with a Triplemate spectrometer. Scattering was excited via an Ar⁺ laser ($\lambda = 488$ nm).

The Raman spectrum of the pristine DWCNTs showed a low intensity D band at 1347 cm⁻¹ (Figure 4 (b), curve 1) indicating the efficiency of the purification method, which eliminated most of the amorphous carbon from the sample. After fluorination, the intensity of the D band increased due to the appearance of sp³-hybridized carbon atoms, which are involved in the covalent CF-bonding. In the low-frequency region (100-400 cm⁻¹) the Raman spectrum of pristine DWCNTs exhibited two groups of radial breathing modes (RBM) (Figure 1(a), curve 1). The lines at ca. 305.0, 288.9, and 225.9 cm⁻¹ correspond to inner tubes with diameters 0.79, 0.84, and 1.08 nm, while the peaks at ca. 200.7, 178.7, and 160.7 cm⁻¹ are due to outer tubes with diameters 1.23, 1.39, and 1.55 nm (diameters obtained using the equation from Ref. 25). Although only DWCNTs with these diameters show up at the given excitation energy, other diameters will also be present in the sample. SWCNTs in the sample could also contribute to the RBMs at higher frequencies. After fluorination, the intensity in the radial breathing region decreased. However, in the spectra of DWCNTs fluorinated by CF₄ plasma and BrF₃ three lines were clearly visible in the 210-320 cm⁻¹ range, which can undoubtedly be attributed to the inner shells of DWCNTs. We note that the frequency of these lines was slightly different for both fluorinated samples as

well as compared to the position of the corresponding lines in the spectrum of the pristine sample. This shows differences in the surroundings of the inner shells in the non-modified and DWCNTs fluorinated by different methods. The RBM corresponding to the scattering from the outer tubes was suppressed in the spectra of all fluorinated samples excluding the spectrum of the plasma fluorinated DWCNTs which shows a low-intensity peak at 179 cm^{-1} (Fig. 1(a), curve 2).

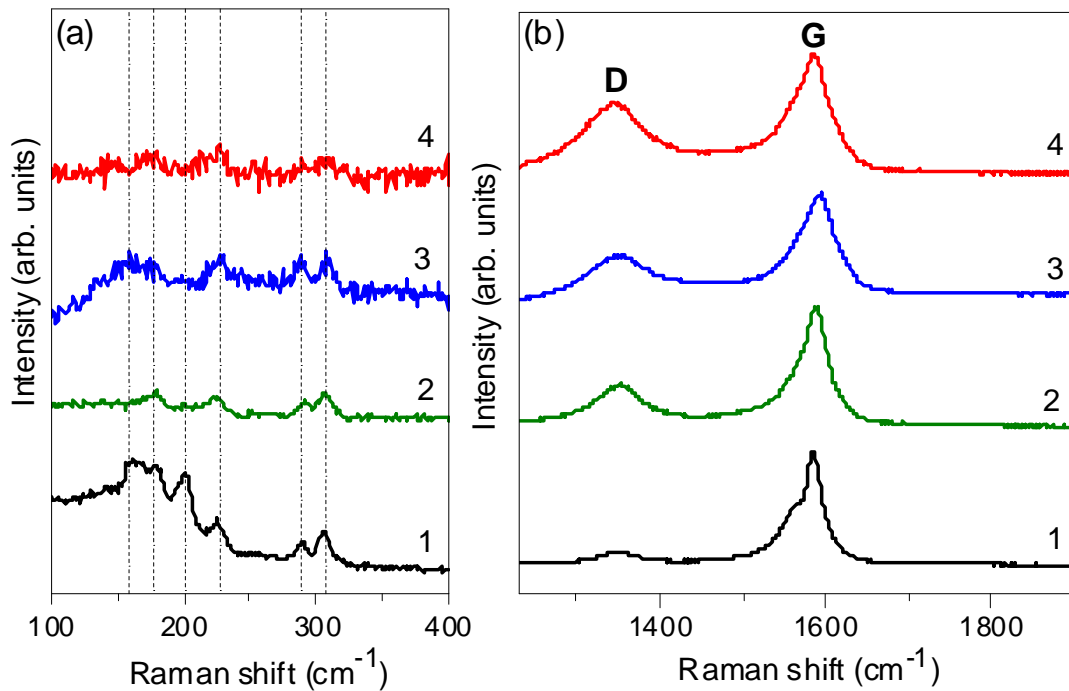


Figure 4. Low-frequency (a) and high-frequency (b) Raman scattering of DWCNT samples: pristine (1), fluorinated by CF_4 plasma (2), fluorinated by BrF_3 at room temperature (3), fluorinated by F_2 at 200°C (4).